J. Phys. B: At. Mol. Opt. Phys. 26 (1993) 2575–2587. Printed in the UK

A hyperspherical close-coupling calculation of photoionization from the He atom, Li^+ and C^{4+} ions: II. Between the $N = 2$ and $N = 3$ thresholds

Bin Zhou and C D Lin

Department of Physics, Kansas State University, Manhattan, Kansas 66506, USA

Received 11 February 1993

Abstract. We report an extensive calculation of photoionization cross sections of the He atom and He-like ions, Li^+ and C^{4+}, using the hyperspherical close-coupling (HSCC) method for photon energies between the $N = 2$, 3 thresholds. Rich resonance structures in the spectra are readily identified with the autoionizing doubly excited states associated with the $N = 3$ manifold. Some systematic trends in the photoionization spectra with the nuclear charge are uncovered and discussed.

1. Introduction

Photoionization cross sections of helium in the energy region between the $N = 2$ and $N = 3$ thresholds have been studied experimentally by measuring the total absorption cross sections, or the spectrum of the ejected electrons. Theoretically the spectrum in this energy region has been examined by a number of methods where the resonances and partial cross sections are calculated to compare with experimental measurements. In the preceding paper (Zhou *et al* 1993, to be referred to as I hereafter), we described the hyperspherical close coupling (HSCC) method for calculating photoionization cross sections and reported the results of photoionization from He, Li^+ and C^{4+} in the energy range below the $N = 2$ threshold. In the present paper we report results obtained in the higher energy region between the $N = 2$ and $N = 3$ thresholds. The same notations used in I will be adopted here. As mentioned in I, for the energy range below the $N = 2$ threshold I_2 there have been some systematic theoretical studies on the photoionization spectra of He-like systems. Above I_2, no such comparative work on the dependence of photoionization cross section and resonance parameters as functions of the nuclear charge exists. Most of the experimental works so far have concentrated only on the helium atom (Woodruff and Samson 1982, Dhez and Ederer 1973, Lindle *et al* 1987, Zubek *et al* 1989). The only experimental information regarding positive He-like ions in this energy range are fragmentary results of resonance positions and autoionization widths of some doubly excited states obtained from collision experiments. With the availability of ions from ECR or EBIS ion sources from different laboratories, photoabsorption studies of positive ions are becoming increasingly possible. The results presented in this paper may serve to stimulate experimentalists for carrying out such measurements.

A careful and extensive theoretical study of the photoionization spectra of He in the energy range between I_2 and I_3 has been done recently by Moccia and Spizzo (1991). Rather than attempting to give every detail of the spectra we shall compare the calculated

0953-4075/93/162575+13$07.50

photoionization cross sections, both total and partial, of the He-like ions of different Z to see how the changing nuclear Coulomb interaction affects the photoionization spectrum.

In the energy region between the $N = 2$ and 3 threshold there are four outgoing channels (1sϵp, 2sϵp, 2pϵs and 2pϵd). Besides the total cross section σ_{tot}, partial cross sections σ_j corresponding to different open channels can be calculated and compared with experiments. Moreover, in this energy range there are five series of autoionizing $^1P^o$ doubly excited states from the $N = 3$ manifold, designated by the ${}_N(K, T)_n^A$ quantum numbers, as ${}_3(1, 1)_n^+$, ${}_3(-1, 1)_n^+$ ($n = 3, 4, \ldots$), and ${}_3(2, 0)_n^-$, ${}_3(0, 0)_n^-$, ${}_3(-2, 0)_n^0$ ($n = 4, 5, \ldots$).

In section 2, the procedure of analysing resonance structures in both total and partial photoionization cross sections is explained. Results and discussion are presented in section 3, where the Z dependence of photoionization spectra and related physical parameters for autoionizing states is studied. A brief summary and conclusion is given in section 4.

2. Analysis of resonances

Energy positions E_r and autoionization widths Γ of the prominent resonances corresponding to doubly excited states with $A = +1$ are obtained by fitting the Fano profile (equation (31) in I) with the calculated total photoionization cross section σ_{tot}. Energy positions of other states (with $A = -1, 0$) are estimated simply by zooming in the local resonance energy region. Since these resonances are extremely weak and narrow in width (at least two orders of magnitude smaller than the major ones) the energy positions thus determined are still quite accurate.

For energies above the $N = 2$ threshold $I\!P_2$, more than one ionization channel is open and partial cross sections corresponding to different final continuum states are obtained. Since the Fano formula is only suitable for the *total* cross section in the neighbourhood of a resonance, one can no longer use equation (31) in I to fit partial cross sections. Starace (1977) derived an expression for the partial photoionization cross section in the proximity of a resonance. In the present work, for energies between the $I\!P_2$ and the $I\!P_3$, we have fitted partial cross sections of all outgoing channels 1sϵp, 2sϵp, 2pϵs, 2pϵd, in the neighbourhood of the ${}_3(1, 1)_3^+$ resonance, with the formula given by Starace (1977)

$$\sigma_j(E) = \frac{\sigma_0^j}{1+\epsilon^2}\left(\epsilon^2 + 2\epsilon\left[q\mathrm{Re}(\alpha_j) - \mathrm{Im}(\alpha_j)\right] + 1 - 2q\mathrm{Im}(\alpha_j) - 2\mathrm{Re}(\alpha_j) + (q^2+1)|\alpha_j|^2\right) \tag{1}$$

where σ_0^j is the background of the partial cross section for the jth channel, q is the usual Fano shape parameter and $\epsilon = 2(E\text{-}E_r)/\Gamma$ with Γ as the total autoionization width of the doubly excited state. The complex parameter α_j, which is to be determined from fitting the partial cross section σ_j of channel j to (1), is expressed as (Kemeny *et al* 1977)

$$\alpha_j = \left(\frac{2\pi}{\Gamma}\right)\frac{\langle\psi_{DES}|H|\psi_E^j\rangle}{\langle\psi_E^j|z_1+z_2|\psi_I\rangle}\left[\sum_{j'}\langle\psi_{DES}|H|\psi_E^{j'}\rangle\langle\psi_E^{j'}|z_1+z_2|\psi_I\rangle\right] \tag{2}$$

where ψ_I is the initial state wavefunction, ψ_{DES} the wavefunction of the doubly excited state and ψ_E^j the final state wavefunction in channel j. The summation on j' is over all open channels.

Furthermore, knowing that $\sigma_0^j = \text{const}E|\langle\psi_E^j|z_1 + z_2|\psi_I\rangle|^2$ and $\sigma_0 = \sum_j \sigma_0^j$, from equation (32), (33) in I and (2), one can obtain a simple relation

$$\left(\frac{\Gamma_j}{\Gamma}\right) = \left(\frac{\sigma_0^j}{\sigma_0}\right)\left(\frac{|\alpha_j|^2}{\rho^2}\right). \tag{3}$$

From (2) and (3), $|\alpha_j|^2$ is just the fraction of the resonance in the partial cross section σ_j, analogous to ρ^2 for the total cross section σ_{tot}. From (3), one can deduce the partial width Γ_j using parameters obtained from fitting the total and partial cross sections.

It should be pointed out that the branching ratios obtained from (3) may not add up exactly to one since parameters on the right hand side of equation (3) are extracted from fitting the calculated partial cross sections. In this work, the partial widths obtained from (3) are renormalized by using

$$\Gamma_j = \Gamma_j / I \qquad \text{where } I = \sum_j \left(\frac{\Gamma_j}{\Gamma}\right) \tag{4}$$

although the identity I is close to one in all cases considered here, as will be discussed in more detail in the next section.

3. Results and discussion

Before we proceed to the result, it should be mentioned that photon energy segments between $N = 2$ and $N = 3$ thresholds for the three elements are located in very different spectroscopic regions, with 65.41–72.97 eV for He, 167.48–184.49 eV for Li^+ and 759.92–827.95 eV for C^{4+}.

3.1. Total cross section σ_{tot}

3.1.1. Photoionization spectra. In figure 1, the total cross sections σ_{tot} for all three elements are shown, as a function of the scaled energy $E^* = (E - IP_N)/(Z-1)^2$ with $N = 3$ and E as the total energy of the two-electron system. $E^* = 0$ corresponds to the $N = 3$ threshold. Note that the $N = 2$ thresholds according to this scale are at -0.27778, -0.15625 and -0.1000 for He, Li^+ and C^{4+} respectively. Only the prominent resonances are labelled, with the simplified notation K_n^A.

From the spectra of the total cross section shown in figure 1, three main features are noted:

(i) In all three elements the most dominant resonances belong to the series 1_n^+, in accordance with the expectation that only those states with $K = (N-2)$ are predominantly populated in photoabsorption. Resonances of the series $(-1)_n^+$ are much smaller but are still conspicuous in figure 1, while resonances from other three series are extremely weak and narrow such that many of them cannot be clearly identified in figure 1.

(ii) The magnitude of the total cross section decreases sharply with increasing Z. For instance, at $E^* = -0.07$ the spectra intensity drops from about 1.0 Mb in He to about 0.085 Mb in C^{4+}.

(iii) Resonances of the same n from different series gradually cluster together as a group as Z increases from 2 to 6. This is more clearly illustrated in figure 2, where the detail of resonances near $n = 4$, 5 is depicted. In figure 2, all the resonances for $n = 4$ including

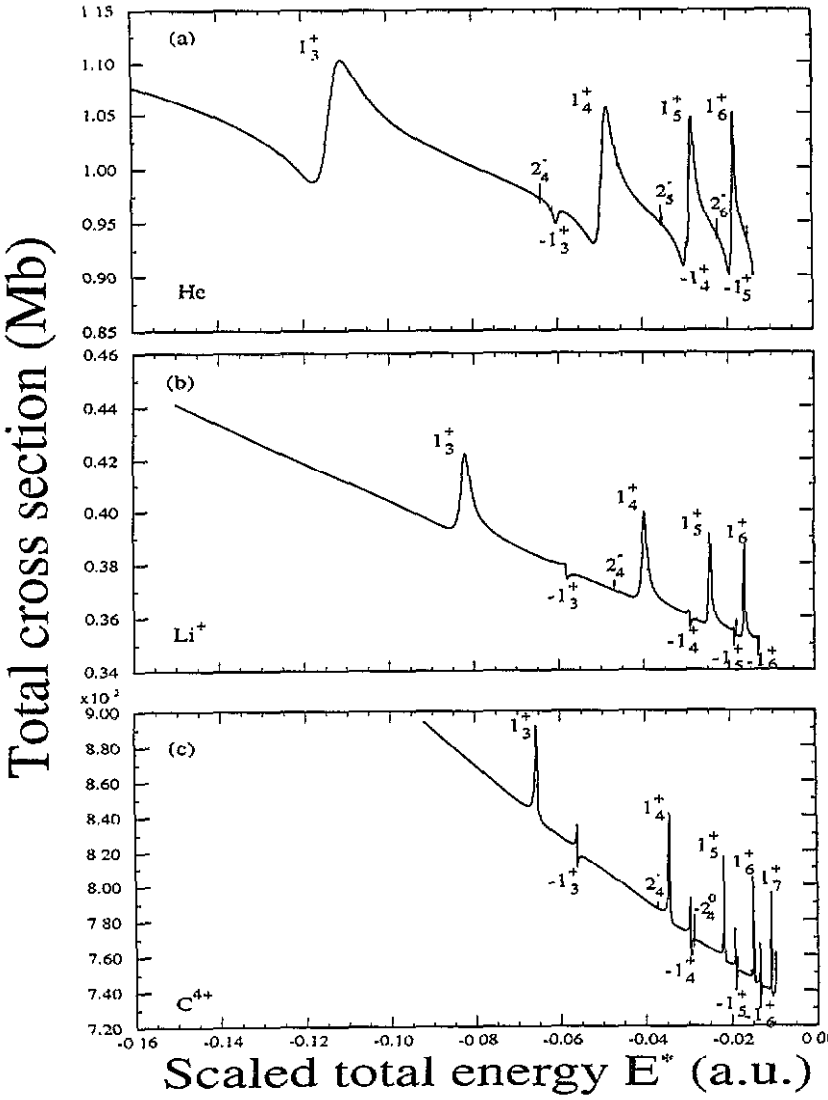

Figure 1. Total photoionization cross section between the $N = 2$ and 3 threshold plotted against the scaled energy E^*: (*a*) for He; (*b*) Li^+; (*c*) C^{4+}.

the weakest one, $(-2)_4^0$, are identified. In the case of He, resonances from three adjacent n (= 4,5,6) series are intermixed with each other in this region; specifically, the resonance $(-1)_4^+$ is very close to and strongly interferes with 1_5^+ while $(-2)_4^0$ locates between 0_5^- and 2_6^- on the higher energy shoulder of 1_5^+. In Li^+, $(-1)_4^+$ has moved below 2_5^-, the lowest member of $n = 5$ resonances, while $(-2)_4^0$ still lies above 2_5^- but below 1_5^+ and 0_5^-. For C^{4+}, all members of $n = 4$ resonances have moved together and located at the lower energy side from those of $n = 5$ which have formed their own group. From figure 1 and 2, it is clear that as Z increases, energies of doubly excited states with the same n approach $E_n^* = -1/(2n^2)$, the electron–electron interaction splits the energies within the manifold into substructures in the ascending order: 2_n^-, 1_n^+, 0_n^-, $(-1)_n^+$, $(-2)_n^0$, from the largest K to the smallest, as seen in figure 1 and 2. The quantum number K represents different

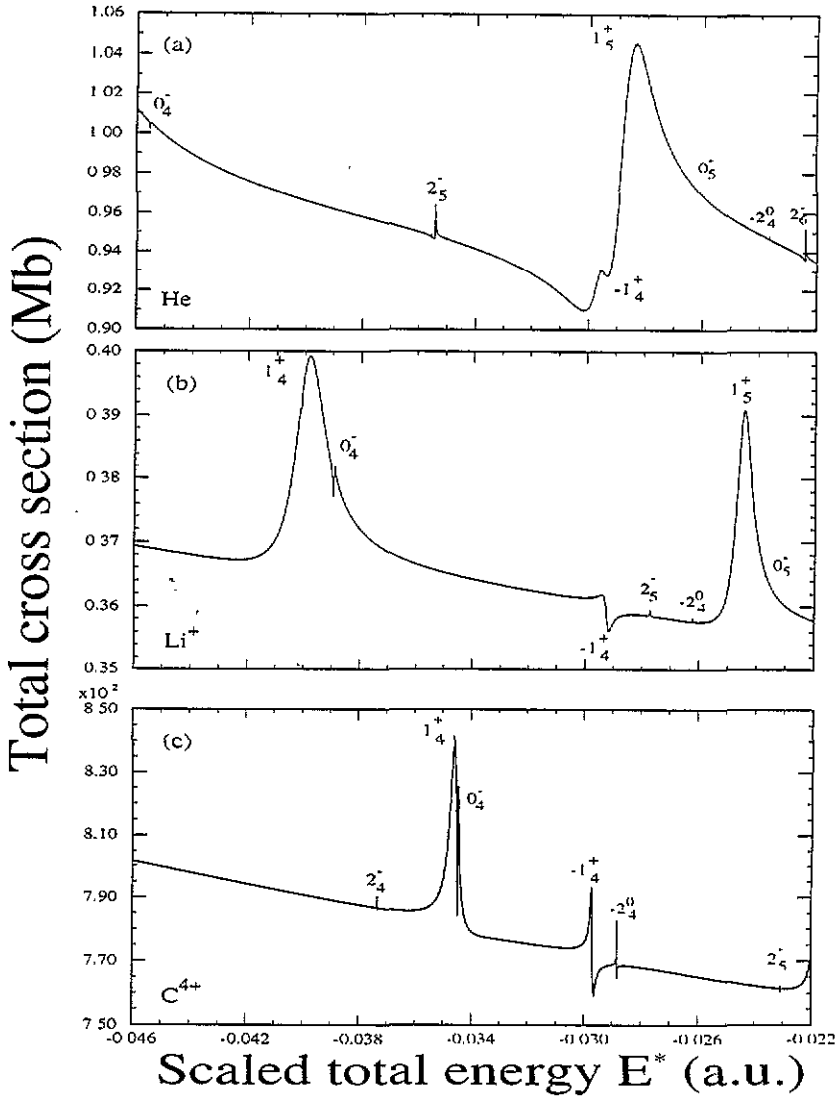

Figure 2. The close-up of the photoionization spectra showing the resonance structures near the $n = 4, 5$ region.

polarization states of the inner electron in the field from the outer one.

3.1.2. Resonance positions and widths. Energy positions E_r of doubly excited states up to $n = 7$ between $I\!P_2$ and $I\!P_3$ and total autoionization widths Γ of the major series 1_n^+, obtained in the present calculation for all three elements, are listed in tables 1–3. The present results are compared with results from other theoretical calculations (Moccia and Spizzo 1991, Lipsky *et al* 1977, Bachau *et al* 1991, Ho 1979, Ho and Callaway 1985, Chen 1992). For He (table 1), energy positions obtained in this work are in the best agreement with the result of the complex coordinate rotation method (CCR) (Ho 1979, Ho and Callaway 1985). They are also in very good agreement with results predicted by other theories, including the truncated diagonalization method (TD) (Lipsky *et al* 1977), the pseudo-potential–Feshbach method (PPF) (Bachau *et al* 1991), the L^2 basis method (LB) (Moccia and Spizzo 1991), and

Table 1. Energy positions and widths $-E_r$ (Γ) in au of He $^1P^o$ states between the $N = 2$ and $N = 3$ threshold.

$_N(K,T)^A_n$	PPP[a,e]	TD[b]	CCR[c]	LB[d,f,g]	SP[e]	Present work
$_3(1,1)^+_3$	0.3357 (9.56E−3)	0.3350	0.3356 (7.00E−3)	0.3354 (6.76E−3)	0.3346	0.3355 (6.96E−3)
$_3(2,0)^-_4$	0.2860 (4.78E−5)	0.2859	0.2860 (2.80E−5)	0.2858 (3.22E−5)	0.2860	0.2861
$_3(-1,1)^+_3$	0.2828 (1.76E−3)	0.2820	0.2828 (1.45E−3)	0.2824 (1.38E−3)	0.2828	0.2825
$_3(1,1)^+_4$	0.2712 (4.04E−3)	0.2707	0.2712 (3.10E−3)	0.2707 (3.01E−3)	0.2709	0.2713 (3.24E−3)
$_3(0,0)^-_4$	0.2675 (1.65E−5)	0.2675	0.2676 (1.00E−5)	0.2673 (2.15E−5)	0.2675	0.2677
$_3(2,0)^-_5$	0.2574 (3.53E−5)	0.2573	0.2574 (1.50E−5)	0.2574 (2.19E−5)	0.2574	0.2577
$_3(-1,1)^+_4$	0.2516 (9.19E−4)	0.2514	0.2516 (5.00E−4)	0.2511 (6.69E−4)	0.2512	0.2514
$_3(1,1)^+_5$	0.2505 (1.58E−3)	0.2504	0.2508 (1.20E−3)	0.2505 (1.07E−3)	0.2504	0.2509 (1.25E−3)
$_3(0,0)^-_5$	0.2478 (1.98E−5)	0.2481	0.2483	0.2481 (1.01E−5)	0.2480	0.2484
$_3(-2,0)^0_4$	0.2446 (9.92E−6)	0.2455	0.2456	0.2451 (5.55E−8)	0.2449	0.2459
$_3(2,0)^-_6$		0.2443		0.2444 (1.32E−5)		0.2446
$_3(1,1)^+_6$		0.2406		0.2407 (0.76E−3)		0.2413 (0.65E−3)
$_3(-1,1)^+_5$		0.2409		0.2406 (2.19E−4)		0.2410
$_3(0,0)^-_6$		0.2392		0.2392 (5.81E−6)		0.2394
$_3(-2,0)^0_5$		0.2380		0.2379 (1.85E−7)		0.2382
$_3(2,0)^-_7$		0.2374		0.2374 (8.31E−6)		0.2376

[a] Bachau *et al* (1991), the pseudo-potential Feshbach method.
[b] Lipsky *et al* (1977), the truncated diagonalization method.
[c] Ho (1979), Ho and Callaway (1985), the complex coordinate rotation method.
[d] Moccia and Spizzo (1991), the L^2 basis method.
[e] Chung and Davis (1980), the saddle-point method.
[f] The conversion of 1 au (^{4}He) = 27.207 696 eV is used.
[g] The ground state energy E_0 is assumed to be −2.903 72 au.

Table 2. Energy positions and widths $-E_r$ (Γ) in au of Li^+ $^1P^o$ states between the $N = 2$ and $N = 3$ thresholds.

$_N(K,T)^A_n$	PPP[a,d]	TD[b]	CCR[c]	Present work
$_3(1,1)^+_3$	0.8297 (0.0114)	0.8284	0.8288 (0.010)	0.8289 (0.0101)
$_3(-1,1)^+_3$	0.7320 (2.46E−3)	0.7300	0.7329 (2.50E−3)	0.7330
$_3(2,0)^-_4$	0.6872 (6.62E−5)	0.6870		0.6874
$_3(1,1)^+_4$	0.6598 (6.62E−3)	0.6584		0.6597 (5.27E−3)
$_3(0,0)^-_4$	0.6555 (8.82E−5)	0.6552		0.6557
$_3(-1,1)^+_4$	0.6161 (8.82E−4)	0.6153		0.6172
$_3(2,0)^-_5$	0.6103 (5.15E−5)	0.6101		0.6108
$_3(-2,0)^0_4$	0.6012 (5.15E−6)	0.6040		0.6049
$_3(1,1)^+_5$	0.5975 (3.49E−3)	0.5966		0.5981 (2.62E−3)
$_3(0,0)^-_5$	0.5929 (3.42E−5)	0.5927		0.5935
$_3(-1,1)^+_5$		0.5742		0.5756
$_3(2,0)^-_6$		0.5724		0.5731
$_3(-2,0)^0_5$		0.5691		0.5701
$_3(1,1)^+_6$		0.5650		0.5660 (1.41E−3)
$_3(0,0)^-_6$		0.5622		0.5629
$_3(-1,1)^+_6$		0.5520		0.5528
$_3(2,0)^-_7$		0.5511		0.5517

[a] Bachau *et al* (1991), the pseudo-potential Feshbach method.
[b] Lipsky *et al* (1977), the truncated diagonalization method.
[c] Ho (1979), the complex coordinate rotation method.
[d] The conversion of 1 au (^{7}Li) = 27.209 536 eV is used.

the saddle-point technique (Chung and Davis 1980). The widths of the 1^+_n series obtained

Table 3. Energy positions and widths $-E_r$ (Γ) in au of C^{4+} $^1P^o$ states between the $N = 2$ and $N = 3$ thresholds.

$_N(K,T)^A_n$	PPF[a]	CI[b]	CCR[c]	Present work
$_3(1,1)^+_3$	3.643 (0.0143)	3.6401	3.6403 (0.0140)	3.6402 (0.0142)
$_3(-1,1)^+_3$	3.399 (3.57E−3)	3.3953	3.4042 (3.90E−3)	3.4029 (3.78E−3)
$_3(2,0)^-_4$	2.932 (6.99E−5)	2.9321		2.9328
$_3(1,1)^+_4$	2.865 (8.46E−3)	2.8624		2.8648 (8.05E−3)
$_3(0,0)^-_4$	2.861 (6.99E−4)	2.8596		2.8618
$_3(-1,1)^+_4$	2.739 (1.69E−3)	2.7347		2.7421 (1.64E−3)
$_3(-2,0)^0_4$	2.710 (3.02E−5)	2.7161		2.7207
$_3(2,0)^-_5$	2.575 (5.88E−5)	2.5754		2.5769
$_3(1,1)^+_5$	2.544 (4.78E−3)	2.5409		2.5449 (3.84E−3)
$_3(0,0)^-_5$	2.534 (9.19E−5)	2.5335		2.5358
$_3(-1,1)^+_5$		2.4754		2.4816 (0.97E−3)
$_3(-2,0)^0_5$		2.4668		2.4720
$_3(2,0)^-_6$		2.3900		2.3922
$_3(1,1)^+_6$		2.3700		2.3742 (2.05E−3)
$_3(0,0)^-_6$		2.3643		2.3671
$_3(-1,1)^+_6$		2.3326		2.3379 (0.59E−3)
$_3(-2,0)^0_6$		2.3276		2.3323
$_3(2,0)^-_7$		2.2813		2.2836

[a] Bachau *et al* (1991), the pseudo-potential Feshbach method.
[b] Chen (1992), the configuration interaction method.
[c] Ho (1979), the complex coordinate rotation method.

are in very good agreement with results of the CCR method (Ho 1979, Ho and Callaway 1985) and of the LB method (Moccia and Spizzo 1991), while the widths given by the PPF method (Bachau *et al* 1991) are considerably larger than others. For Li^+ (table 2), the energy positions and total widths obtained are in excellent agreement with those from the CCR method (Ho 1979) which however only calculated the first two resonance states. The energy positions are also in quite good agreement with results of the PPF method (Bachau *et al* 1991) except for the $(-2)^0_4$ state. The widths predicted by the PPF method are generally larger than the present results. The energy positions given by the TD method are consistently higher than the present results. In C^{4+} (table 3), we have also presented autoionization widths of the less dominant $A = +$ series $(-1)^+_n$. Our result still has the best agreement with the result of the CCR method for the first two resonances. The present result agrees reasonably well with results of the PPF method (Bachau *et al* 1991) and of the CI method (Chen 1992), in terms of energy positions. The widths obtained for both + series are in fair agreement with those of the PPF method (Bachau *et al* 1991) wherever the latter are available.

In the case of He (table 1), we want to point out that the present result shows an intriguing reversion of relative energy positions at $n = 5$ between the $(-1)^+_n$ and 1^+_{n+1} states which are extremely close to each other. This reversion has also been shown in the LB calculation (Moccia and Spizzo 1991) (but not in the result obtained using the TD method (Lipsky *et al* 1977)) and has been subject to scrutiny more recently by Wintgen and Delande (1992).

3.1.3. Z-dependence of σ_0, Γ, ρ^2 and q of 1^+_3 resonance. In table 4, E_r, Γ and parameters q, σ_0, a, ρ^2, obtained from fitting the Fano profile (equation(31) in I) to the total cross section spectra near the most prominent resonance $_3(1,1)^+_3$, are listed for the three elements. In the case of He, results from two experiments (Dhez and Ederer 1973, Lindle *et al* 1987) and

Table 4. Fano parameters for the $^1P^o\ {}_3(1, 1)_3^+$ resonance. The numbers in parentheses represent experimental uncertainties.

	ω_r (eV)	Γ (eV)	q	σ_0 (Mb)	a (eV^{-1})	ρ^2
He						
Present work	69.876[a]	0.189[a]	1.26	1.030	−0.0452	0.0421
Moccia and Spizzo (1991)	69.874	0.197	1.24	1.034	−0.0448	0.047
Lindle *et al* (1987)	69.917[b]	0.178[b]	1.30(5)	0.989(30)	−0.047 55	0.057(5)
Dhez and Ederer (1973)	69.919	0.132(14)	1.36(20)	0.957(30)	0(fixed)	0.012(3)
Li^+						
Present work	175.530[c]	0.275[c]	3.68	0.393	−0.0158	5.49E−3
C^{4+}						
Present work	783.283[d]	0.386[d]	−10.13	0.084	−0.0036	5.86E−4

[a] The conversion of 1 au (^{4}He) = 27.207 696 eV is used.
[b] Taken from Woodruff and Samson (1982).
[c] The conversion of 1 au (^{7}Li) = 27.209 536 eV is used.
[d] The conversion of 1 au (^{12}C) = 27.210 418 eV is used.

the L^2 basis calculation of Moccia and Spizzo (1991) are compared with the present results. The resonance energy position in terms of photon energy ω_r from the present calculation, which differs from Moccia and Spizzo's value only by 2 meV, is more than 40 meV smaller than the experimental values of both Lindle *et al* (1987) and of Dhez and Ederer (1973). Our results for Γ, q, σ_0, a, ρ^2 are in very good agreement with the experiment of Lindle *et al* (1987) and the calculation of Moccia and Spizzo (1991). The parameters obtained by Dhez and Ederer (1973) with the background slope a fixed to zero, are also in the close range of other results. For Li^+ and C^{4+} ions, no other works are available for comparison.

In table 4 the parameter σ_0 decreases (roughly $\sim Z^{-2}$) while Γ increases monotonically, as Z changes from 2 to 6. The Z^{-2} behaviour of σ_0 can be understood in the same way as described in I, because out of the four open channels the contribution from the $1s\epsilon p$ channel is by far the most dominant one to σ_0. As a result, the background of the total cross section will have almost the same Z^{-2} dependence of $\sigma_0^{1s\epsilon p}$. The reasoning given in I for the behaviour of autoionization widths with Z is rather general and can be applied to any doubly excited states and to partial widths as well. In other words, one expects an autoionization width, total or partial, of any given doubly excited state in a two-electron atomic system, to increase monotonically toward a finite limit as the nuclear charge increases.

Despite similarities described above, there are several striking differences between the ${}_2(0, 1)_2^+$ resonance and the ${}_3(1, 1)_3^+$ resonance. For ${}_2(0, 1)_2^+$ the parameter $\rho^2 \equiv 1$, but from table 4 one finds that ρ^2 for ${}_3(1, 1)_3^+$ is close to zero and decreases sharply with increasing Z. A simple scale analysis of its expression in terms of matrix elements (equation (33) of I) indicates that ρ^2 does not have any explicit Z dependence. However, as pointed out by Fano and Cooper (1965), the correlation coefficient ρ associated with an autoionizing state can be thought of as the overlap between two parts of the continuum: one part into which the doubly excited state autoionizes and another part into which the ground state is directly excited by the dipole transition. In the case of the ${}_3(1, 1)_3^+$ state, these two parts correspond mainly to the ($2s\epsilon p$, $2p\epsilon s$ and $2p\epsilon d$) states and the $1s\epsilon p$ state respectively. The interaction between these two different parts in the continuum, which is measured by their mutual overlap and is essentially the intershell interaction in the continuum, is generally quite small and diminishes as the nuclear charge increases. Thus the parameter ρ^2 for the ${}_3(1, 1)_3^+$ resonance is very small for all three elements and rapidly decreases to zero with increasing Z.

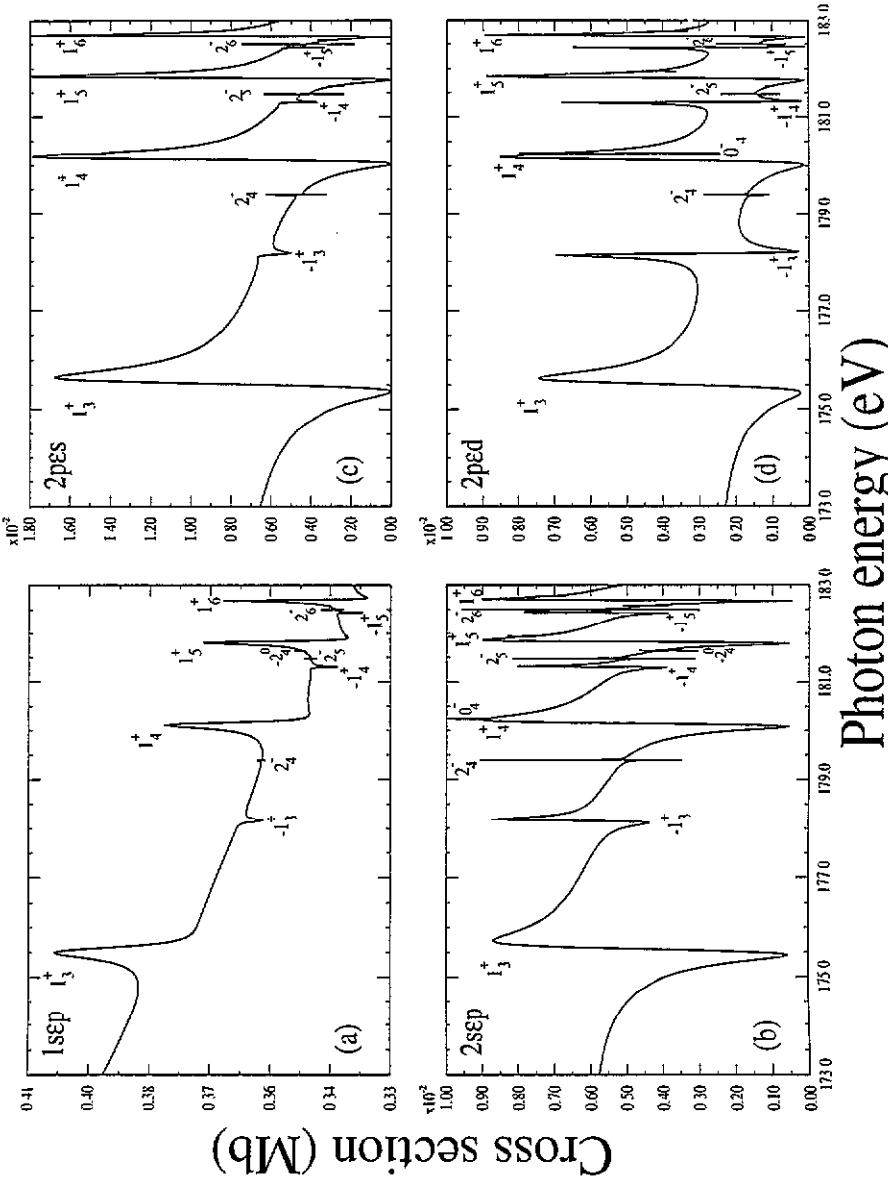

Figure 3. Partial cross sections for Li^+ between the $N = 2$ and 3 thresholds: (*a*) 1sεp; (*b*) 2sεp; (*c*) 2pεs; (*d*) 2pεd.

Also shown in table 4, we note that the q parameter of the ${}_3(1, 1)_3^+$ resonance changes drastically from 1.26 for He to -10.13 for C^{4+}, reflecting the change of shape from a 'window' type resonance in He to a more Lorentzian-like resonance for for C^{4+}. This drastic behaviour of q for the ${}_3(1, 1)_3^+$ state might not be seen as a total surprise, considering that more than one continuum channels are open and their presence as summations further complicates the expression of q (equation (34) in I).

3.2. Partial cross sections σ_j

In figure 3, a representative example of all four partial cross sections for the Li^+ ion is given. As expected, $1s\epsilon p$ is the dominant channel which is primarily populated by the direct dipole transition. Partial cross sections of the other three channels, $\sigma_{2s\epsilon p}$, $\sigma_{2p\epsilon s}$ and $\sigma_{2p\epsilon d}$, where the residual core is being left in the $N = 2$, are more than one order of magnitude smaller. In these $N = 2$ partial cross sections, resonances from the weak series $(-1)_n^+$, 2_n^-, 0_n^-, $(-2)_n^0$ are more conspicuous due to the weaker background.

In figures 3(*b*)–(*d*), the profiles of 1_n^+ resonances in different $N = 2$ channels resemble each other with positive 'q' numbers, whereas in the $1s\epsilon p$ channel they appear to be quite different, with a negative 'q'. The appearance of the $(-1)_n^+$ resonances in the $N = 2$ cross sections changes dramatically from channel to channel. The same phenomenon also occurs in $N = 2$ outgoing channels of He and C^{4+}.

As Z changes, the partial cross section for a given channel also changes significantly. This is demonstrated in figure 4, where partial cross sections $\sigma_{2p\epsilon d}$ for He and C^{4+} are shown for photon energies near $n = 4$, 5 resonances. Note the logarithmic scale is used for the cross section. Other than the change of resonance positions described in 3.1.1 and declining intensities, the structure of resonances also displays rather significant changes from He to C^{4+}. In $\sigma_{2p\epsilon d}$ of He, both 1_n^+, $(-1)_n^+$ states appear as typical window type resonances, whereas they appear with sizable upward peaks as well as downward ones in the C^{4+} spectrum.

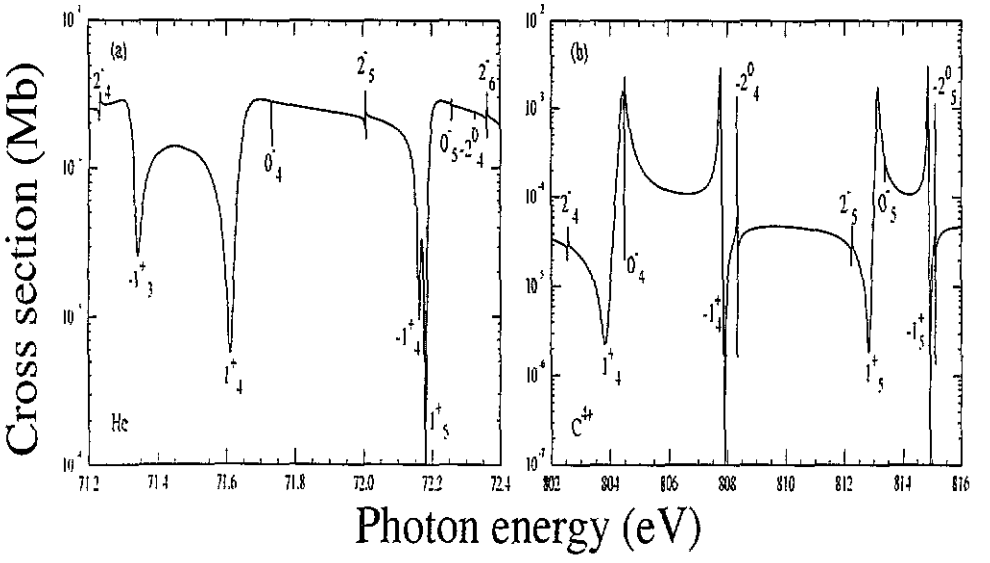

Figure 4. Partial cross section $\sigma_{2p\epsilon d}$ between the $N = 2$ and 3 thresholds of: (*a*) He; (*b*) C^{4+}.

Table 5. Comparison of Starace parameters and branching ratios for the $^1P^o\ _3(1,1)_3^+$ resonance of He. The upper rows are results from the present calculation and the lower ones are from Lindle *et al* (1987). The numbers in the parentheses represent experimental uncertainties.

j	σ_0^j (Mb)	Re(α_j)	Im(α_j)	$100\times(\Gamma_j/\Gamma)$
1sϵp	0.9313	−0.016 27	−0.026 77	2.11
	0.892(5)	0.000(15)	−0.036(19)	2.0(16)
2sϵp	0.0316	0.398	0.227	15.31
	0.030(4)	0.46(17)	0.13(28)	12(7)
2pϵs	0.0472	0.706	0.172	57.35
	0.045(7)	0.76(9)	0.30(15)	58(16)
2pϵd	0.0232	0.666	0.442	34.16
	0.022(3)	0.76(9)	0.30(15)	28(7)

Table 6. Starace parameters and partial linewidths for the $^1P^o\ _3(1,1)_3^+$ resonance.

	j	σ_0^j (Mb)	Re(α_j)	Im(α_j)	$\lvert\alpha_j\rvert^2$	Γ_j^a	Γ_j^b	Γ_j^c	Γ_j^d
He	1sϵp	0.9313	−1.627E−2	−2.677E−2	9.814E−4	0.135E−3	0.13E−3		
	2sϵp	0.0316	0.398	0.227	0.210	0.978E−3	0.95E−3		
	2pϵs	0.0472	0.706	0.172	0.528	3.665E−3	3.60E−3		
	2pϵd	0.0232	0.666	0.442	0.639	2.183E−3	2.08E−3		
Li^+	1sϵp	0.3778	−7.028E−3	−6.672E−3	9.391E−5	0.167E−3		0.11E−3	
	2sϵp	0.0053	0.239	5.289E−2	0.060	1.47E−3		1.55E−3	
	2pϵs	0.0065	0.380	0.168	0.173	5.21E−3		3.30E−3	
	2pϵd	0.0026	0.433	0.295	0.275	3.27E−3		2.83E−3	
C^{4+}	1sϵp	8.315E−2	2.670E−3	−1.133E−3	8.413E−6	0.20E−3		0.15E−3	0.12E−3
	2sϵp	3.50E−4	−0.145	−0.118	0.035	3.37E−3		3.06E−3	4.41E−3
	2pϵs	3.86E−4	−0.229	−0.121	0.067	7.15E−3		6.15E−3	6.99E−3
	2pϵd	0.63E−4	−0.455	−0.140	0.227	3.60E−3		4.13E−3	2.76E−3

[a] Present work.
[b] Moccia and Spizzo (1991).
[c] Chen (1992).
[d] Bachau *et al* (1991).

We have fitted all four partial cross sections $\sigma_{1s\epsilon p}$, $\sigma_{2s\epsilon p}$, $\sigma_{2p\epsilon s}$ and $\sigma_{2p\epsilon d}$ of the three elements in the neighbourhood of the $_3(1,1)_3^+$ resonance with the formula (1) proposed by Starace (1977). In table 5, the background cross section σ_0^j, the complex parameter α_j and the branching ratio (without the renormalization) obtained from fitting the partial cross sections of He are compared with the experimentally extracted counterparts by Lindle *et al* (1987). The results agree very well with the experimental data, especially for branching ratios. The final results of all three elements are summarized in table 6. Note the branching ratios Γ_j/Γ are obtained independently from fitting each individual partial cross section. The quantity I in (4), the sum of all branching ratios, is close to one in the present work, with its value at 1.089, 1.016, 1.023 for He, Li^+ and C^{4+} respectively, implying good quality of the fitting. The partial widths Γ_j for the present work shown in table 6 have been renormalized using equation (4). They are compared with partial widths predicted by other theoretical works (Bachau *et al* 1991, Moccia and Spizzo 1991, Chen 1992). The widths obtained in the present work are in excellent agreement with results obtained using the LB method (Moccia and Spizzo 1991) for He while they are in qualitative agreement with results of the CI calculation (Chen 1992) for both Li^+ and C^{4+}. For all three elements,

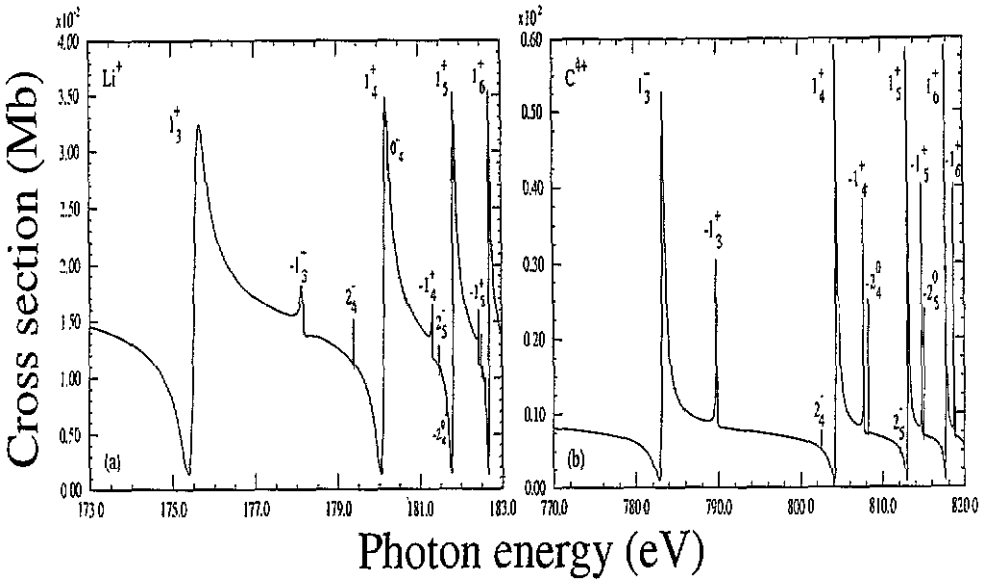

Figure 5. The total cross sections for all $N = 2$ outgoing channels $\sigma_{N=2}$ ($= \sigma_{2s\epsilon p} + \sigma_{2p\epsilon s} + \sigma_{2p\epsilon d}$) between the $N = 2$ and 3 thresholds, as functions of the photon energy: (*a*) Li^+; (*b*) C^{4+}.

$2p\epsilon s$ is shown to be the largest autoionizing channel while $1s\epsilon p$ the smallest channel. In the case of C^{4+}, the PPF calculation (Bachau *et al* 1991) predicted $\Gamma_{2s\epsilon p}$ is nearly twice $\Gamma_{2p\epsilon d}$ whereas both the present calculation and the CI calculation (Chen 1992) indicate $\Gamma_{2s\epsilon p}$ should be slightly smaller than $\Gamma_{2p\epsilon d}$. The present result appears to show that for all three elements, $\Gamma_{2p\epsilon s}$ has the largest value, followed by $\Gamma_{2p\epsilon d}$, $\Gamma_{2s\epsilon p}$, whereas $\Gamma_{1s\epsilon p}$ is about one order of magnitude smaller than others.

Some systematics of parameters from table 6 as functions of Z are noted and explained in the following.

(i) The background σ_0^j for different channels has different Z dependence: $\sigma_0^{1s\epsilon p}$ decreases with $\sim Z^{-2}$ while $\sigma_0^{2s\epsilon p}$, $\sigma_0^{2p\epsilon s}$ decrease more like $\sim Z^{-4}$ ($\sigma_0^{2p\epsilon d}$ appears to decrease even faster). The Z^{-2} dependence of $\sigma_0^{1s\epsilon p}$ has been explained in I. The Z^{-4} dependence of the $N = 2$ cross sections can be understood in a similar fashion from the CI point of view by expressing the initial state wavefunction

$$|\psi_I\rangle = a_1|1s1s\rangle + a_2|1s2s\rangle + \ldots$$

For example, $\sigma_0^{2s\epsilon p} = \text{const}\ E|\langle\psi_E^{2s\epsilon p}|z_1 + z_2|\psi_I\rangle|^2 = \text{const}\ E|\langle 2s\epsilon p|z_1 + z_2|(a_1|1s1s\rangle + a_2|1s2s\rangle + \ldots)|^2$. Since only the matrix element from the second term (the first one is the major configuration) in the initial state wavefunction does not vanish, we may rewrite $\sigma_0^{2s\epsilon p} = \text{const}\ a_2^2[E|\langle 2s\epsilon p|z_1 + z_2|1s2s\rangle|^2]$. The quantity in the square bracket has Z^{-2} dependence and the CI coefficient a_2 has Z^{-1} dependence. Therefore $\sigma_0^{2s\epsilon p}$ will have Z^{-4} dependence. The same can be applied to other $N = 2$ channels.

(ii) The parameter $|\alpha_j|^2$ for each channel decreases monotonically with increasing Z, implying the reduced fraction from the autoionization of the doubly excited state in each partial cross section. Noticeably, $|\alpha_{1s\epsilon p}|^2$ seems to go to zero whereas $|\alpha_{N=2}|^2$ ($|\alpha_{2p\epsilon d}|^2$ in particular) towards some non-zero limits as Z varies from 2 to 6.

(iii) The partial width Γ_j to any given channel j increases monotonically with the nuclear charge Z, just like the total width Γ.

Finally, in the hope of stimulating experiments on photoionization of positive He-like ions in this energy range, in figure 5 we present the total cross section $\sigma_{N=2}(= \sigma_{2s\epsilon p} + \sigma_{2p\epsilon s} + \sigma_{2p\epsilon d})$ of all $N = 2$ outgoing channels for both Li^+ and C^{4+} ions. It should be noted that figure 5 and all other figures shown in this paper have assumed an infinite energy resolution. If convoluted with the finite resolution of an experiment, most of those sharp and narrow resonances might be smeared off. Despite low spectral intensities, it should be possible to observe resonances of 1_n^+, $(-1)_n^+$ series and maybe other resonances in the photoionization spectra of ions, in the sense that the requirement for the energy resolution is less stringent because widths and energy separations for autoionizing doubly excited states of positive ions are larger than those of He.

4. Conclusions

Using the HSCC method described in I, we have carried out the calculation of photoionization cross sections for the two-electron systems of He, Li^+ and C^{4+} in the energy range between $N = 2$ and 3 thresholds. Both the total and partial cross sections are obtained and analysed, using Fano and Starace's formulae respectively. Similar to what was found in I, the spectral (both total and partial) intensities sharply decrease and resonances of the same n quantum number group together as the nuclear charge increases. The intensities of partial cross section decline with different Z dependence, with $\sigma_0^{N=2} \sim Z^{-4}$ and $\sigma_0^{N=1} \sim Z^{-2}$. As a result of diminishing intershell interactions in the doubly excited state, the total as well as partial autoionization widths of the 1_3^+ resonance increase monotonically with increasing Z. Furthermore, it is shown that due to diminishing intershell electron–electron interactions in the final continuum state the parameter ρ^2 for 1_3^+ resonance rapidly decreases to zero as Z is increased.

Acknowledgments

This work was supported in part by the US Department of Energy, Office of Basic Energy Research, Division of Chemical Sciences.

References

Bachau H, Martin F, Riera A and Yanez M 1991 *At. Data Nucl. Data Tables* **48** 167
Chen Z 1992 Private communication
Chung K T and Davis B F 1980 *Phys. Rev.* A **22** 835
Dhez P and Ederer D L 1973 *J. Phys. B: At. Mol. Phys.* **6** L59
Fano U and Cooper J W 1965 *Phys. Rev.* **137** 1364
Ho Y K 1979 *J. Phys. B: At. Mol. Phys.* **12** 387
Ho Y K and Callaway J 1985 *J. Phys. B: At. Mol. Phys.* **18** 3481
Kemeny P C, Samson J A R and Starace A F 1977 *J. Phys. B: At. Mol. Phys.* **10** L201
Lindle D W, Ferrett T A, Heimann P A and Shirley D A 1987 *Phys. Rev.* A **36** 2112
Lipsky L, Anania R and Conneely M J 1977 *At. Data Nucl. Data Tables* **20** 127
Moccia R and Spizzo P 1991 *Phys. Rev.* A **43** 2199
Starace A F 1977 *Phys. Rev.* A **16** 231
Wintgen D and Delande D 1992 Preprint
Woodruff P R and Samson J A 1982 *Phys. Rev.* A **25** 848
Zhou B, Lin C D, Tang J Z, Watanabe S and Matsuzawa M 1993 *J. Phys. B: At. Mol. Opt. Phys.* **26** 2555
Zubek M, King G C, Rutter P M and Read F H 1989 *J. Phys. B: At. Mol. Opt. Phys.* **22** 3411